Arch. Mech., **52**, 4–5, pp. 589–607, Warszawa 2000

Elastic-plastic stress-strain analysis of notches under non-proportional loading paths

Dedicated to Professor Zenon Mróz on the occasion of his 70th birthday

G. GLINKA ([1]), A. BUCZYŃSKI ([2]), A. RUGGERI ([3])

([1]) *University of Waterloo, Department of Mechanical Engineering, Waterloo, Ontario N2L 3G1, Canada*

([2]) *Warsaw University of Technology, Institute of Heavy Machinery Engineering, ul. Narbutta 85, 02524 Warsaw, Poland*

([3]) *INSA of Toulouse, Department of Mechanical Engineering, 135 Avenue de Rangueil, 31077 Toulouse Cedex 4, France*

AN ANALYTICAL METHOD for calculating notch tip stresses and strains in elastic-plastic bodies subjected to non-proportional loading sequences is discussed in the paper. The method is based on the incremental formulation relating the hypothetical linear elastic and elastic-plastic strain energy densities at the notch tip, and the material stress-strain behavior simulated according to the Mróz-Garud cyclic plasticity model. Two formulations involving the strain energy density and the complementary strain density are discussed in the paper, and they appear to give the lower and the upper bound estimates for the elastic-plastic notch tip strains. Each formulation consists of a set of incremental algebraic equations that can easily be solved for elastic-plastic stress and strain increments, knowing the increments of the hypothetical elastic notch tip stress history and the material stress-strain curve. The validation of the proposed model against finite element data obtained for non-proportional loading is also presented. The method is particularly suitable for fatigue life analysis of notched bodies subjected to multiaxial cyclic loading paths.

Key Words: notches, nonproportional loading, inelastic strains

Notations

$\Delta\varepsilon_{22}$	normal strain increment in the critical plane
$\Delta\varepsilon_{ij}^{p}$	plastic strain increments
δ_{ij}	Kronecker delta, $\delta_{ij} = 1$ for $i = j$ and $\delta_{ij} = 0$ for $i \neq j$
$\Delta\varepsilon_{jk}^{e}$	elastic strain increments

$\Delta\varepsilon_{jk}^{E}$	elastic-plastic strain increments according to ESED method
Δ_{jk}^{N}	elastic-plastic strain increments according to Neuber's rule
$\Delta\varepsilon_{eq}^{pE}$	equivalent plastic strain increment according to ESED method
$\Delta\varepsilon_{eq}^{pN}$	equivalent plastic strain increment according to Neuber's rule
$\Delta\sigma_{ik}^{e}$	increments of pseudo-elastic stress components
$\Delta\sigma_{ik}^{E}$	actual elastic-plastic stress increments according to ESED method
$\Delta\sigma_{ik}^{N}$	actual elastic-plastic stress increments according to Neuber's rule
$\Delta\sigma_{eq}^{N}$	equivalent stress increment according to Neuber's rule
ΔS_{ij}^{e}	symmetric tensor of the pseudo-elastic stress state
ΔS_{ij}^{E}	symmetric tensor of elastic-plastic stress state acording to the strain energy density increment
ΔW_{ij}^{e}	tensor of elastic strain energy density increment
ΔW_{ij}^{E}	tensor of elastic-plastic strain energy density increment
$\Delta\Omega_{ij}^{e}$	tensor of elastic total strain energy density increment
$\Delta\Omega_{ij}^{N}$	tensor of elastic-plastic total strain energy density increment
ΔT_{ij}^{e}	symmetric tensor of elastic total strain energy density increment
ΔT_{ij}^{N}	symmetric tensor of elastic-plastic total strain energy density increment
E	modulus of elasticity
ε_{eq}^{p}	equivalent plastic strain
ε_{eq}^{pE}	equivalent plastic strain determined by the ESED method
ε_{ij}^{E}	elasto-plastic notch-tip strains obtained from the ESED method
ε_{ij}^{e}	notch tip strain components obtained from linear elastic analysis
ε_{ij}^{N}	elasto-plastic notch-tip strains obtained by the Neuber method
ε_{ij}^{p}	plastic components of the notch-tip strain tensor
ε_{n}	nominal strain
ESED	equivalent strain energy density
ν	Poisson's ratio
P	axial load
T	torque
R	radius of a cylindrical specimen
S_{ij}	deviatoric stress components
σ_{eq}	equivalent stress
σ_{ij}^{a}	actual stress tensor components in the notch tip
σ_{ij}^{e}	notch tip stress tensor components obtained from linear elastic analysis
σ_{ij}^{E}	notch tip stress tensor components obtained from the ESED model
σ_{ij}^{N}	notch tip stress tensor components obtained from the Neuber solution
σ_{n}	nominal stress
σ_{n}^{P}	nominal (average) stress in the net cross-section due to axial load P
σ_{o}	parameter of the material stress-strain curve (yield limit)
σ_{Y}	yield limit
t	wall thickness
τ_{n}	nominal shear stress in the net cross-section

1. Introduction

FATIGUE ANALYSES of machine and structure components require a detailed elastic-plastic stress-strain analysis at critical locations, such as notches, where the stress concentration occurs. In most cases the stress state in the notch tip region is multiaxial. However, if one of the stress components is the dominant one, it is often assumed that uniaxial stress or plane strain state prevails at the notch tip. Such an approximation might be satisfactory in a wide variety of practical applications but there are cases where all the stress and strain components have to be accounted for. This is particularly true when several loads are applied simultaneously and the stress components at the notch root change non-proportionally. For example, axles and shafts may experience combined out-of-phase torsion and bending loads.

The main focus of this paper is to present a method for calculating multiaxial elastic-plastic stresses and strains in notched bodies subjected to proportional and non-proportional loading histories.

2. Loading histories

Fatigue cracks most often initiate at the notch tip where the highest stress concentration occurs. Therefore, most fatigue analyses are focused on the determination of fatigue life of the material volume adjacent to the notch tip, which is under the effect of the local notch tip stress-strain history. The notch tip stresses and strains are dependent on the notch geometry, the material properties and the loading history applied to the notched body. If the various cyclic stress components are in phase and change proportionally with each other, the loading is called *proportional*. When the applied load causes the directions of the principal stresses and the ratio of the principal stress magnitudes to change after each load increment, the loading is termed *non-proportional*.

If plastic yielding takes place at the notch tip then almost always the stress path in the notch tip region is non-proportional, regardless of whether the remote loading is proportional or not. However, the remote proportional loading does not make the notch tip stress tensor rotate and therefore, it makes the stress analysis easier in spite of the fact that some non-proportionality of the notch tip stress history may occur.

The non-proportional loading/stress paths are usually defined by successive increments of appropriate load/stress parameters and therefore all calculations have to be carried out incrementally.

3. The stress state at the notch tip

If the dimensions and external loads applied to a body are such that the plane stress state dominates in the body, then the stress state at the notch tip is uni-axial (Fig. 1a), providing that the surface at the notch tip is stress-free. If the notched body is in the state of plane strain (Fig. 1b), the notch tip stress-strain state is fully characterized by only two principal non-zero stress components and two non-zero principal strain components.

For the case of general multiaxial loading applied to a notched body, the state of stress near the notch tip is tri-axial. However, the stress state at the notch tip is bi-axial because of the stress-free notch tip surface (Fig. 1c). Since equilibrium of the element at the notch tip must be maintained, i.e. $\sigma_{23} = \sigma_{32}$ and $\varepsilon_{23} = \varepsilon_{32}$, there are in general three non-zero stress components and four non-zero strain components. There are seven unknowns altogether and a set of seven independent equations is required for the determination of all the stress and strain components at the notch tip. The material constitutive relationships provide four equations, leaving three additional relationships to be established.

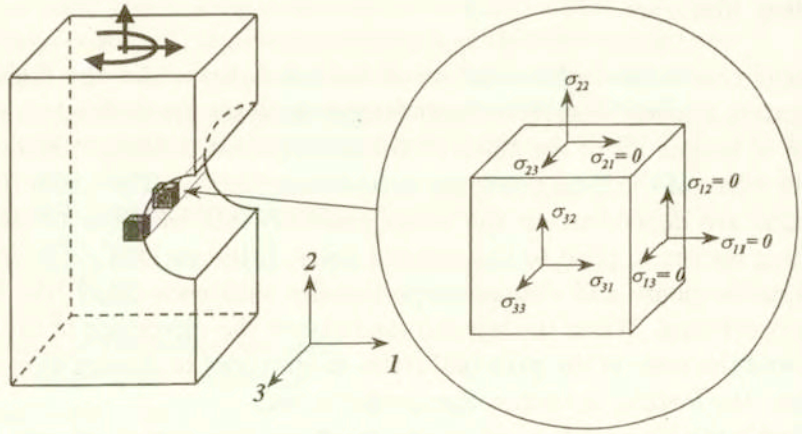

(a) Plane Stress

$$\sigma_{ij} = \begin{bmatrix} 0 & 0 & 0 \\ 0 & \sigma_{22} & 0 \\ 0 & 0 & 0 \end{bmatrix} \qquad \varepsilon_{ij} = \begin{bmatrix} \varepsilon_{11} & 0 & 0 \\ 0 & \varepsilon_{22} & 0 \\ 0 & 0 & \varepsilon_{33} \end{bmatrix}$$

(b) Plane Strain

$$\sigma_{ij} = \begin{bmatrix} 0 & 0 & 0 \\ 0 & \sigma_{22} & 0 \\ 0 & 0 & \sigma_{33} \end{bmatrix} \qquad \varepsilon_{ij} = \begin{bmatrix} \varepsilon_{11} & 0 & 0 \\ 0 & \varepsilon_{22} & 0 \\ 0 & 0 & 0 \end{bmatrix}$$

(c) General

$$\sigma_{ij} = \begin{bmatrix} 0 & 0 & 0 \\ 0 & \sigma_{22} & \sigma_{23} \\ 0 & \sigma_{32} & \sigma_{33} \end{bmatrix} \qquad \varepsilon_{ij} = \begin{bmatrix} \varepsilon_{11} & 0 & 0 \\ 0 & \varepsilon_{22} & \varepsilon_{23} \\ 0 & \varepsilon_{32} & \varepsilon_{33} \end{bmatrix}$$

FIG. 1. Stress state at a notch tip (notation): a) body in plane stress; b) body in plane strain; c) general bi-axial stress state.

4. Material constitutive model

In the case of proportional or nearly proportional notch tip stress path, the Hencky total deformation equations of plasticity can be used in the analysis,

$$\varepsilon_{ij} = \frac{1+\nu}{E}\sigma_{ij} - \frac{\nu}{E}\sigma_{kk}\delta_{ij} + \frac{3}{2}\frac{\varepsilon^p_{eq}}{\sigma_{eq}}S_{ij}. \tag{4.1}$$

The material constitutive model of incremental plasticity, most frequently used in the case of non-proportional loading paths, is the Prandtl-Reuss flow rule associated with the von Mises plastic yielding criterion. For an isotropic body, the Prandtl-Reuss relationship can be expressed as:

$$\Delta\varepsilon_{ij} = \frac{1+\nu}{E}\Delta\sigma_{ij} - \frac{\nu}{E}\Delta\sigma_{kk}\delta_{ij} + \frac{3}{2}\frac{\Delta\varepsilon^p_{eq}}{\sigma_{eq}}S_{ij}. \tag{4.2}$$

The multiaxial incremental stress-strain relation (4.2) is obtained from the uniaxial stress-strain curve by relating the equivalent plastic strain increment to the equivalent stress increment, such that

$$\Delta\varepsilon^p_{eq} = \frac{df(\sigma_{eq})}{d\sigma_{eq}}\Delta\sigma_{eq}. \tag{4.3}$$

The function, $\varepsilon^p_{eq} = f(\sigma_{eq})$, is identical to the plastic strain-stress relationship obtained under uniaxial loading.

5. The load-notch tip stress-strain relations

The load in the case of notched bodies is usually represented by the nominal or reference stress being proportional to the remote applied load or by the pseudo-elastic stresses at the notch tip which would exist there in the absence of plasticity. In the case of notched bodies in plane stress or plane strain state, the relationship between the load and the elastic-plastic notch tip strains and stresses is most often approximated by the Neuber rule [1] or the Equivalent Strain Energy Density (ESED) equation [2]. It was shown later [3, 4] that both methods can be extended to multiaxial proportional and non-proportional modes of loading. However, the multiaxial Neuber and ESED [3, 4] models are not the only methods for determination of multiaxial elastic-plastic strain and stress states at the notch tip. HOFFMAN and SEEGER [5] and BARKEY *et al.* [6] also proposed similar methods. All of the approximate methods consist, in general, of two parts, namely: the constitutive equations and the relationships linking the fictitious linear elastic stress-strain state $(\sigma^e_{ij}, \varepsilon^e_{ij})$ at the notch tip with the actual elastic-plastic stress-strain response $(\sigma^a_{ij}, \varepsilon^a_{ij})$ as shown in Fig. 2.

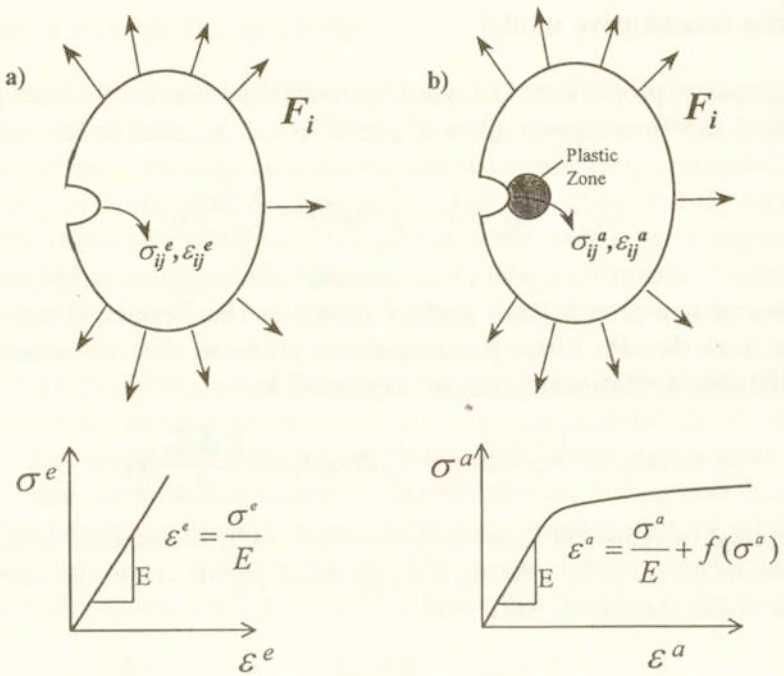

FIG. 2. The linear elastic and elastic-plastic strain and stress states in geometrically identical bodies.

The Neuber and the ESED rule [2, 3] for proportional loading, where the Hencky stress-strain relationships are applicable, can be written in the form of Eqs. (5.1) and (5.2), respectively,

$$\sigma_{ij}^e \varepsilon_{ij}^e = \sigma_{ij}^N \varepsilon_{ij}^N, \tag{5.1}$$

$$\int_0^{\varepsilon_{ij}^e} \sigma_{ij}^e d\varepsilon_{ij}^e = \int_0^{\varepsilon_{ij}^E} \sigma_{ij}^E d\varepsilon_{ij}^E. \tag{5.2}$$

The ESED method is based on the equivalence of the strain energy density as shown in Fig. 3a. The Neuber rule represents the equality of total strain energy shown graphically in Fig. 3b. Detail discussion of the incremental Neuber rule (5.3) and the ESED equation (5.4) and their use for calculating the elastic-plastic notch tip strains and stresses can be found in reference [4]:

– Incremental Neuber's rule

$$\sigma_{ij}^e \Delta\varepsilon_{ij}^e + \varepsilon_{ij}^e \Delta\sigma_{ij}^e = \sigma_{ij}^N \Delta\varepsilon_{ij}^N + \varepsilon_{ij}^N \Delta\sigma_{ij}^N. \tag{5.3}$$

– Incremental ESED equation

$$\sigma_{ij}^e \Delta\varepsilon_{ij}^e = \sigma_{ij}^E \Delta\varepsilon_{ij}^E. \tag{5.4}$$

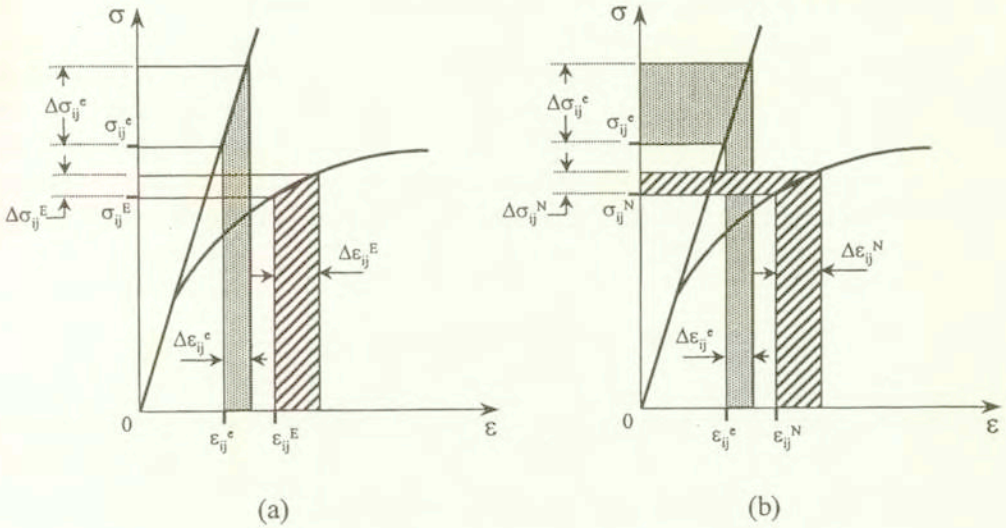

FIG. 3. Graphical representation of: a) Incremental ESED method; b) Incremental Neuber's rule.

The overall energy equivalence in the form of Eq. (5.3) or (5.4), relating the pseudo-elastic and the actual elastic-plastic notch tip strains and stresses, has been accepted in general, but the additional conditions necessary for the complete formulation of the problem are being the subject of controversy. HOFFMAN and SEEGER [5] assumed that the ratio of the actual principal strains at the notch tip is to be equal to the ratio of fictitious elastic principal strain components while BARKEY *et al.* [6] suggested to use the ratio of principal stresses. The data presented by MOFTAKHAR [7] indicate that the accuracy of the analysis based on the principal stress or principal strain ratio at the notch tip depended on the constraint at the notch tip. Unfortunately, it is very difficult to define criteria enabling the proper choice of those additional conditions.

The accuracy of the additional energy equations presented by SINGH *et al.* [4] seems to be less dependent on the geometry and constraint conditions at the notch tip and therefore, the analyst is not forced to make any arbitrary decisions while using them. However, they have a theoretical drawback indicated by CHU [8] because they do not have tensor properties and thus the estimated elastic-plastic notch tip strains and stresses depend on the system of coordinates. The dependence is not very strong and with suitably chosen system of reference, it could be sufficiently accurate for engineering applications. Nevertheless, it is possible to formulate an axis-invariant system of equations similar to those discussed in references [4, 8].

6. Multiaxial equivalent strain energy density equations

The strain energy density equations can be written in terms of equality of components of two tensors ΔW_{ij}^e and ΔW_{ij}^E representing inner products of the stress tensor σ_{ik} and the corresponding strain increment tensor $\Delta\varepsilon_{kj}$. The strain energy density increment, ΔW_{ij}^e, called here the strain energy density tensor induced by the pseudo-elastic stress and strain increments at the notch tip (Fig. 2a) can be determined as:

$$\Delta W_{ij}^e = \sigma_{ik}^e \cdot \Delta\varepsilon_{kj}^e. \tag{6.1}$$

The actual strain energy density tensor, ΔW_{ij}^E, resulting from the actual elastic-plastic stress and strain increments at the notch tip (Fig. 2b) can be also determined as the inner product of the current stress tensor and the strain increment tensor,

$$\Delta W_{ij}^E = \sigma_{ik}^E \cdot \Delta\varepsilon_{kj}^E. \tag{6.2}$$

In the case of the notch tip surface free of stress (Fig. 1c), tensors (6.1) and (6.2) can be presented in the matrix form with all elements in the first column and the first row being equal to zero:

$$\Delta W_{ij}^e = \begin{bmatrix} 0 & 0 & 0 \\ 0 & \sigma_{22}^e\Delta\varepsilon_{22}^e + \sigma_{23}^e\Delta\varepsilon_{32}^e & \sigma_{22}^e\Delta\varepsilon_{23}^e + \sigma_{23}^e\Delta\varepsilon_{33}^e \\ 0 & \sigma_{32}^e\Delta\varepsilon_{22}^e + \sigma_{33}^e\Delta\varepsilon_{32}^e & \sigma_{32}^e\Delta\varepsilon_{23}^e + \sigma_{33}^e\Delta\varepsilon_{33}^e \end{bmatrix} \tag{6.3}$$

and

$$\Delta W_{ij}^E = \begin{bmatrix} 0 & 0 & 0 \\ 0 & \sigma_{22}^E\Delta\varepsilon_{22}^E + \sigma_{23}^E\Delta\varepsilon_{32}^E & \sigma_{22}^E\Delta\varepsilon_{23}^E + \sigma_{23}^E\Delta\varepsilon_{33}^E \\ 0 & \sigma_{32}^E\Delta\varepsilon_{22}^E + \sigma_{33}^E\Delta\varepsilon_{32}^E & \sigma_{32}^E\Delta\varepsilon_{23}^E + \sigma_{33}^E\Delta\varepsilon_{33}^E \end{bmatrix}. \tag{6.4}$$

The physical meaning of the diagonal terms in matrix (6.3) and (6.4) is obvious because the two products in each diagonal term represent the strain energy density increments contributed by individual stress components and the corresponding strain increments. The sum of diagonal terms in both tensors represents the increment of the strain energy density. The meaning of the off-diagonal terms is less clear but they can be interpreted as increments of the virtual strain energy density increments analogously to the term used in the virtual energy method well-known in solid mechanics stress/load analyses. The product, $\sigma_{22}^e\Delta\varepsilon_{23}^e$, in the term W_{23}^e in matrix (6.3), can be interpreted as the virtual strain energy increment contributed by stress, σ_{22}^e, on the strain increment, $\Delta\varepsilon_{23}^e$, induced by the shear stress, σ_{23}^e. The second product, $\sigma_{23}^e\Delta\varepsilon_{33}^e$, being a part of the same

term, W^e_{23}, can be analogously considered as the virtual strain energy density increment contributed by the shear stress component, σ^e_{23}, on the normal strain increment, $\Delta\varepsilon^e_{33}$, induced by normal stress components, σ^e_{22} and σ^e_{33}.

Tensors (6.3) and (6.4) are in general non-symmetric. However, they can easily be made symmetric by taking the average of the sum of both off-diagonal terms.

(6.5) $$\Delta S^e_{ij} =$$

$$= \begin{bmatrix} 0 & 0 & 0 \\ 0 & \sigma^e_{22}\Delta\varepsilon^e_{22} + \sigma^e_{23}\Delta\varepsilon^e_{32} & \dfrac{(\sigma^e_{22}+\sigma^e_{33})\Delta\varepsilon^e_{23} + \sigma^e_{23}(\Delta\varepsilon^e_{22}+\Delta\varepsilon^e_{33})}{2} \\ 0 & \dfrac{(\sigma^e_{22}+\sigma^e_{33})\Delta\varepsilon^e_{23} + \sigma^e_{23}(\Delta\varepsilon^e_{22}+\Delta\varepsilon^e_{33})}{2} & \sigma^e_{32}\Delta\varepsilon^e_{23} + \sigma^e_{33}\Delta\varepsilon^e_{33} \end{bmatrix}$$

and

(6.6) $$\Delta S^E_{ij} =$$

$$= \begin{bmatrix} 0 & 0 & 0 \\ 0 & \sigma^E_{22}\Delta\varepsilon^E_{22} + \sigma^E_{23}\Delta\varepsilon^E_{32} & \dfrac{(\sigma^E_{22}+\sigma^E_{33})\Delta\varepsilon^E_{23} + \sigma^E_{23}(\Delta\varepsilon^E_{22}+\Delta\varepsilon^E_{33})}{2} \\ 0 & \dfrac{(\sigma^E_{22}+\sigma^E_{33})\Delta\varepsilon^E_{23} + \sigma^E_{23}(\Delta\varepsilon^E_{22}+\Delta\varepsilon^E_{33})}{2} & \sigma^E_{32}\Delta\varepsilon^E_{23} + \sigma^E_{33}\Delta\varepsilon^E_{33} \end{bmatrix}$$

Analogously to the hypothesis proposed in references [2, 3, 4], it is assumed that the strain energy increments at the notch tip in the pseudo-elastic and the elastic-plastic body (Fig. 2) of identical geometrical shape and subjected to identical loads, are equal. Such a hypothesis can be written in terms of the equality of tensors (6.5) and (6.6),

(6.7) $$\Delta S^e_{ij} = \Delta S^E_{ij}.$$

The hypothesis written in the form of Eq. (6.7) results in three independent equations relating the pseudo-elastic strain and stress components and the actual elastic-plastic stress-strain response at the notch tip in the elastic-plastic body (Fig. 2).

(6.8) $$\sigma^e_{22}\Delta\varepsilon^e_{22} + \sigma^e_{23}\Delta\varepsilon^e_{23} = \sigma^E_{22}\Delta\varepsilon^E_{22} + \sigma^E_{23}\Delta\varepsilon^E_{23},$$

(6.9) $$\sigma^e_{33}\Delta\varepsilon^e_{33} + \sigma^e_{23}\Delta\varepsilon^e_{23} = \sigma^e_{33}\Delta\varepsilon^E_{33} + \sigma^E_{23}\Delta\varepsilon^E_{23},$$

(6.10) $$(\sigma^e_{22}+\sigma^e_{33})\Delta\varepsilon^e_{23} + \sigma^e_{23}(\Delta\varepsilon^e_{22}+\Delta\varepsilon^e_{33}) = (\sigma^E_{22}+\sigma^E_{33})\Delta\varepsilon^E_{23} + \sigma^E_{23}(\Delta\varepsilon^E_{22}+\Delta\varepsilon^E_{33}).$$

Equations (6.8) – (6.10) can be supplemented with four constitutive equations obtained from the general constitutive relationship (4.2).

$$\Delta\varepsilon_{11}^{E} = -\frac{\nu}{E}(\Delta\sigma_{22}^{E} + \Delta\sigma_{33}^{E}) - \frac{1}{2}(\sigma_{22}^{E} + \sigma_{33}^{E})\frac{\Delta\varepsilon_{eq}^{pE}}{\sigma_{eq}^{E}}, \tag{6.11}$$

$$\Delta\varepsilon_{22}^{E} = \frac{1}{2}(\Delta\sigma_{22}^{E} - \nu\Delta\sigma_{33}^{E}) + \frac{1}{2}(2\sigma_{22}^{E} - \sigma_{33}^{E})\frac{\Delta\varepsilon_{eq}^{pE}}{\sigma_{eq}^{E}}, \tag{6.12}$$

$$\Delta\varepsilon_{33}^{E} = \frac{1}{E}(\Delta\sigma_{33}^{E} - \nu\Delta\sigma_{22}^{E}) + \frac{1}{2}(2\sigma_{33}^{E} - \sigma_{22}^{E})\frac{\Delta\varepsilon_{eq}^{pE}}{\sigma_{eq}^{E}}, \tag{6.13}$$

$$\Delta\varepsilon_{23}^{E} = \frac{1+\nu}{E}\Delta\sigma_{23}^{E} + \frac{3}{2}\frac{\Delta\varepsilon_{eq}^{pE}}{\sigma_{eq}^{E}}\sigma_{23}^{E}, \tag{6.14}$$

where:

$$(\sigma_{eq}^{E})^2 = (\sigma_{22}^{E})^2 + (\sigma_{33}^{E})^2 - \sigma_{22}^{E}\sigma_{33}^{E} + 3(\sigma_{23}^{E})^2,$$

$$\Delta\sigma_{eq}^{E} = \frac{(\sigma_{22}^{E} - \sigma_{33}^{E})(\Delta\sigma_{22}^{E} - \Delta\sigma_{33}^{E}) + 3\sigma_{23}^{N}\Delta\sigma_{23}^{N}}{\sigma_{eq}^{N}},$$

$$\Delta\varepsilon_{eq}^{pE} = \frac{df(\sigma_{eq}^{E})}{d\sigma_{eq}^{E}}\Delta\sigma_{eq}^{E}.$$

Equations (6.8) – (6.14) form a set of equations enabling the determination of all the elastic-plastic strains, $(\Delta\varepsilon_{11}^{E}, \Delta\varepsilon_{22}^{E}, \Delta\varepsilon_{33}^{E}, \Delta\varepsilon_{23}^{E})$, and stress increments $(\sigma_{22}^{E}, \sigma_{33}^{E}, \sigma_{23}^{E})$ based on the pseudo-elastic stress history at the notch tip. A graphical representation of the incremental ESED method is shown in Fig. 3a, where the strain energy densities are represented by the vertical bars of the trapezoidal shape whose areas, according to Eqs. (6.8) – (6.9), must be equal.

7. Total strain energy density equations

A set of equations similar to Eqs. (6.8) – (6.10) can also be written in terms of the total strain energy density, i.e. the sum of the strain energy density and the complementary strain energy density, analogously to the well-known Neuber's rule [1]. The tensor representation of the increments of the total strain energy density in the notch tip of linear elastic body (Fig. 2a) can be written as

$$\Omega_{ij}^{e} = \sigma_{ik}^{e} \cdot \Delta\varepsilon_{kj}^{e} + \Delta\sigma_{ik}^{e} \cdot \varepsilon_{kj}^{e}. \tag{7.1}$$

Analogously, the tensor representation of the total strain energy density increments at the notch tip of geometrically identical elastic-plastic body (Fig. 2b) can be written as

$$\Delta\Omega_{ij}^N = \sigma_{ik}^N \cdot \Delta\varepsilon_{kj}^N + \Delta\sigma_{ik}^N \cdot \varepsilon_{kj}^N. \tag{7.2}$$

Tensors (7.1) and (7.2) are non-symmetric but they can be converted into two symmetric tensors T_{ij}^e and T_{ij}^N, respectively. Similarly to the strain energy density tensor (6.1) and (6.2), the sum of the diagonal terms of tensors T_{ij}^e and T_{ij}^N represents the increment of the total strain energy density, i.e., the strain energy density plus the complementary strain energy density. The off-diagonal terms can be interpreted as the virtual strain energy density and the virtual complementary strain energy density, analogously to the formulation discussed above. It is then postulated, similarly to the original Neuber concept, that in the case of localized plastic yielding in the notch tip region the symmetric tensors are equal,

$$\Delta T_{ij}^e = \Delta T_{ij}^N. \tag{7.3}$$

It can be shown that Eq. (7.3) reduces to the well-known Neuber's rule [1, 2] in the case of uni-axial stress state, and to the model proposed by MOFTAKHAR *et al.* [3] for multiaxial proportional loading. Because all the necessary relationships are formulated in terms of tensor equations, it is hoped that the proposed methodology is, contrary to the previous models [4], axis-invariant.

In the case of one surface free of stress, as it often occurs in notches (Fig. 1), the tensorial equation (7.3) leads to three independent equations relating the pseudo-elastic and the elastic-plastic strain and stress increments at the notch tip:

$$\begin{aligned}\sigma_{22}^e\Delta\varepsilon_{22}^e + \Delta\sigma_{22}^e\varepsilon_{22}^e + \sigma_{23}^e\Delta\varepsilon_{23}^e + \Delta\sigma_{23}^e\varepsilon_{23}^e = \sigma_{22}^N\Delta\sigma_{22}^N + \Delta\sigma_{22}^N\varepsilon_{22}^N \\ +\sigma_{23}^N\Delta\varepsilon_{23}^N + \Delta\sigma_{23}^N\varepsilon_{23}^N,\end{aligned} \tag{7.4}$$

$$\begin{aligned}\sigma_{33}^e\Delta\varepsilon_{33}^e + \Delta\sigma_{33}^e\varepsilon_{33}^e + \sigma_{23}^e\Delta\varepsilon_{23}^e + \Delta\sigma_{23}^e\varepsilon_{23}^e = \sigma_{33}^N\Delta\varepsilon_{33}^N + \Delta\sigma_{33}^N\varepsilon_{33}^N \\ +\sigma_{23}^N\Delta\varepsilon_{23}^N + \Delta\sigma_{23}^N\varepsilon_{23}^N,\end{aligned} \tag{7.5}$$

$$\begin{aligned}(\sigma_{22}^e + \sigma_{33}^e)\Delta\varepsilon_{23}^e + (\Delta\sigma_{22}^e + \Delta\sigma_{33}^e)\varepsilon_{23}^e + \sigma_{23}^e(\Delta\varepsilon_{22}^e + \Delta\varepsilon_{33}^e) \\ +\Delta\sigma_{23}^e(\varepsilon_{22}^e + \varepsilon_{33}^e) = (\sigma_{22}^N + \sigma_{33}^N)\Delta\varepsilon_{23}^N + (\Delta\sigma_{22}^N + \Delta\sigma_{33}^N)\varepsilon_{23}^N \\ +\sigma_{23}^N(\Delta\varepsilon_{22}^N + \Delta\varepsilon_{33}^N) + \Delta\sigma_{23}^N(\varepsilon_{22}^N + \varepsilon_{33}^N).\end{aligned} \tag{7.6}$$

Equations (7.4) – (7.6) and the four constitutive equations (7.7) – (7.10) below form a set of seven equations necessary for complete formulation of the notch tip

stress-strain problem.

$$\Delta\varepsilon_{11}^N = -\frac{\nu}{E}(\Delta\sigma_{22}^N + \Delta\sigma_{33}^N) - \frac{1}{2}(\sigma_{22}^N + \sigma_{33}^N)\frac{\Delta\varepsilon_{eq}^{pN}}{\sigma_{eq}^N}, \tag{7.7}$$

$$\Delta\varepsilon_{22}^N = \frac{1}{E}(\Delta\sigma_{22}^N - \nu\Delta\sigma_{33}^N) + \frac{1}{2}(2\sigma_{22}^N - \sigma_{33}^N)\frac{\Delta\varepsilon_{eq}^{pN}}{\sigma_{eq}^N}, \tag{7.8}$$

$$\Delta\varepsilon_{33}^N = \frac{1}{E}(\Delta\sigma_{33}^N - \nu\Delta\sigma_{22}^N) + \frac{1}{2}(2\sigma_{33}^N - \sigma_{22}^N)\frac{\Delta\varepsilon_{eq}^{pN}}{\sigma_{eq}^N}, \tag{7.9}$$

$$\Delta\varepsilon_{23}^N = \frac{1+\nu}{E}\Delta\sigma_{23}^N + \frac{3}{2}\frac{\Delta\varepsilon_{eq}^{pN}}{\sigma_{eq}^N}\sigma_{23}^N, \tag{7.10}$$

where:

$$(\sigma_{eq}^N)^2 = (\sigma_{22}^N)^2 + (\sigma_{33}^N)^2 - \sigma_{22}^N\sigma_{33}^N + 3(\sigma_{23}^N)^2,$$

$$\Delta\sigma_{eq}^N = \frac{(\sigma_{22}^N - \sigma_{33}^N)(\Delta\sigma_{22}^N - \Delta\sigma_{33}^N) + 3\sigma_{23}^N\Delta\sigma_{23}^N}{\sigma_{eq}^N},$$

$$\Delta\varepsilon_{eq}^{pN} = \frac{df(\sigma_{eq}^N)}{d\sigma_{eq}^N}\Delta\sigma_{eq}^N.$$

In the case of uni-axial or plane strain state at the notch tip, the set of seven equations reduces to two equations as proposed originally by NEUBER [1]. The equivalence of the increments of the total strain energy density is graphically shown in Fig. 3b, where the energies are represented by the horizontal and vertical rectangles whose areas are assumed to be equal.

8. Comparison of the calculated elastic-plastic notch tip strains and stresses with finite element data

Comparison of the calculated notch tip stress-strain histories to those obtained by means of the finite element method assessed the accuracy of the proposed incremental Neuber rule. The validation of the ESED method was outside of the scope of this paper. The elastic-plastic results from the finite element analysis of Ref. [4] were obtained using the ABAQUS finite element package. The geometry of the notched element was that of the circumferentially notched bar shown in Fig. 4. The nominal torsional stresses, τ_n, and tensile stresses, σ_{nF}, were determined basing on the net cross-section according to Eq. (8.1).

$$\sigma_{nF} = \frac{F}{\pi(R-t)^2} \quad \text{and} \quad \tau_n = \frac{2T}{\pi(R-t)^3}. \tag{8.1}$$

The basic proportions of the cylindrical component were $\rho/t = 1.0$ and $R/t = 23.333$ resulting in the torsional and tensile stress concentration factor $K_T = \sigma^e_{23}/\tau_n = 1.82$ and $K_P = \sigma^e_{23}/\sigma_{nF} = 2.80$, respectively. The ratio of the notch tip hoop stress to axial stress under tensile loading was $\sigma^e_{33}/\sigma^e_{22} = 0.2179$.

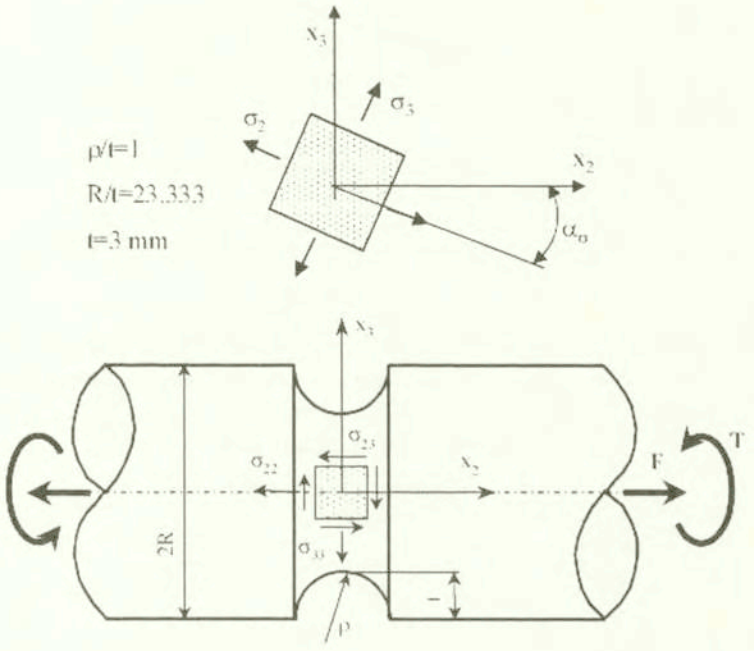

FIG. 4. Geometry and dimensions of the notched bar tested under non-proportional tension and torsion loading.

The linear segments shown in Fig. 5 approximated the material stress-strain curve used in calculations. The curve segments are defined by coordinates $(\varepsilon - \sigma)$ of each transition point, namely: $0-0$, $0.0039-200$ MPa, $0.00317-249$ MPa and $0.029-530$ MPa. The remaining standard elastic constants were $E = 200$ GPa, $\nu = 0.3$, $\sigma_Y = 200$ MPa.

The first set of data was obtained for non-proportional monotonic loading history (no unloading) shown in Fig. 6. The pseudo-elastic axial stress, σ^e_{22}, and the torsional shear stress, σ^e_{23}, at the notch tip represent the loading path. The specimen of Fig. 4 was loaded incrementally from zero to the load level corresponding to $\sigma^e_{22} = 108.89$ MPa and $\sigma^e_{23} = 161.06$ MPa and then the axial stress was further increased to the level of $\sigma^e_{22} = 344.10$ MPa while the shear stress was decreased to $\sigma^e_{23} = 120.78$ MPa, as shown in Fig. 5.

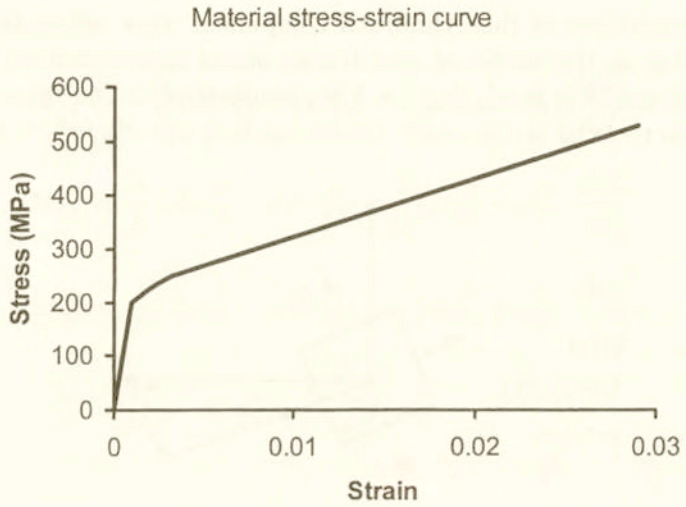

FIG. 5. The three linear segments material stress-strain curve used for the analysis of strain and stresses under the monotonic non-proportional loading path.

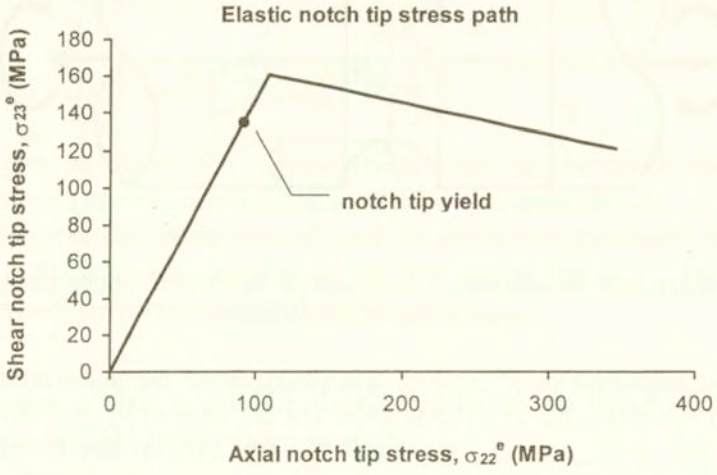

FIG. 6. The monotonic non-proportional torsion-tension load path.

The local pseudo-elastic stress path at the notch tip shown in Fig. 6 was used as the input to calculate the elastic-plastic notch tip stress-strain response. The appropriate 'elastic' stress increments were inputted into Eqs. (7.4) – (7.10) representing the total strain energy density (Neuber) approach. The calculated strains and stresses were subsequently compared with the elastic-plastic finite element data. The strain components, ε_{22} and ε_{23}, and the stress components, σ_{22} and σ_{23}, that were calculated using the method described above, are shown in Figs. 7 and 8. Note that the results from the model and the finite element

analysis are identical in the elastic range. This could be expected since the model converges to the elastic solution in the elastic range. Just beyond the onset of yielding at the notch tip, the strain results that were predicted using the proposed model and the finite element data begin gradually to diverge. However, the method gives reasonably good estimation of the notch tip stress-strain behavior. It can be concluded that the incremental total strain energy density (Neuber) method over-predicts the actual notch tip strains. The investigations up to date have revealed that the actual notch tip strains are always within the band defined by the two methods decribed above, and the average values of the two limits may be used as a good approximation of the actual stress-strain state at the notch tip.

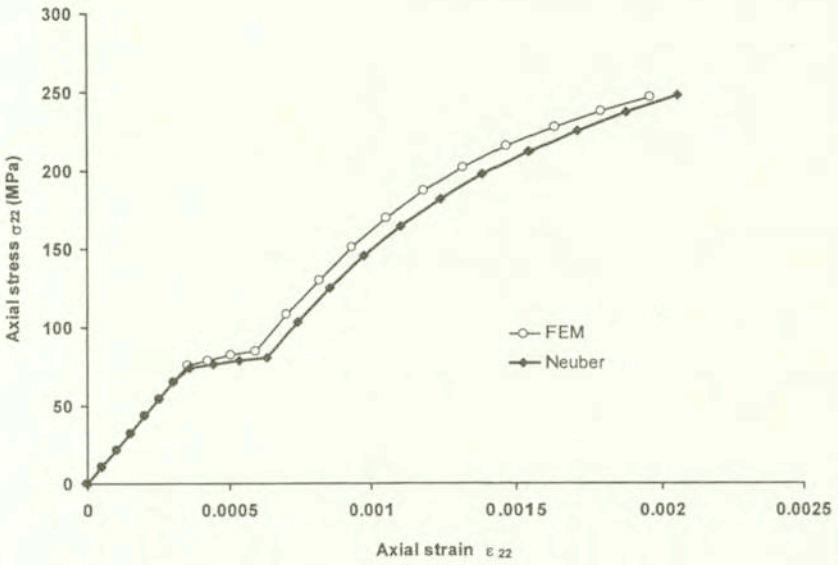

FIG. 7. The axial stress and strain, σ_{22} and ε_{22}, at the notch tip, generated by the monotonic non-proportional loading path.

In order to predict the notch tip stress-strain response of a notched component subjected to multiaxial cyclic loading, the incremental equations discussed above have to be linked with the cyclic plasticity model as described in Ref. [9]. The MRÓZ [10] model modified by GARUD [11] was used with the incremental Neuber model discussed above. The analysis was carried out for a constant amplitude multiaxial proportional cyclic loading history shown in Fig. 9. The loading history is represented by the excursions of three pseudo-elastic stress components. The maximum and minimum stress values were 285.9 and -85.77 MPa for the axial stress σ^e_{22}, 62.30 and -18.69 MPa for the hoop stress σ^e_{33}, and 195.18 and -58.55 MPa for the shear stress σ^e_{23}.

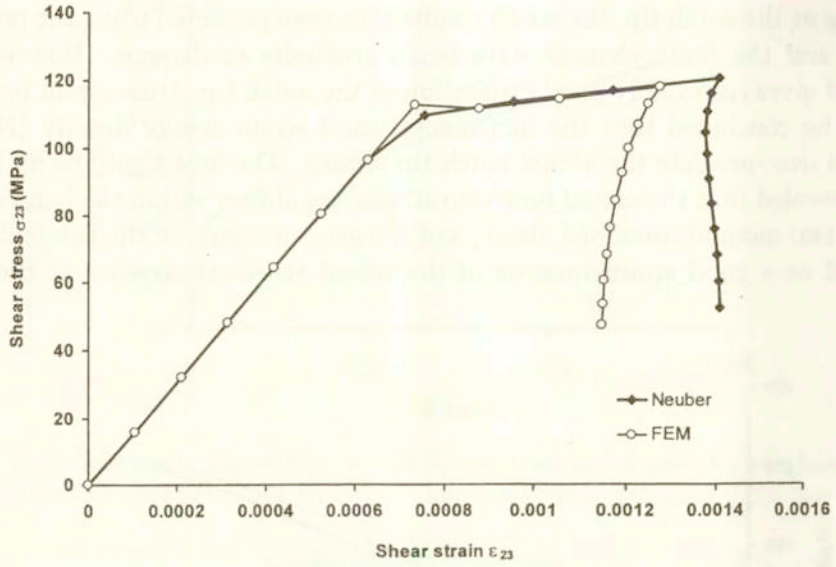

FIG. 8. The shear stress and strain, σ_{23} and ε_{23}, at the notch tip, generated by the monotonic non-proportional loading path.

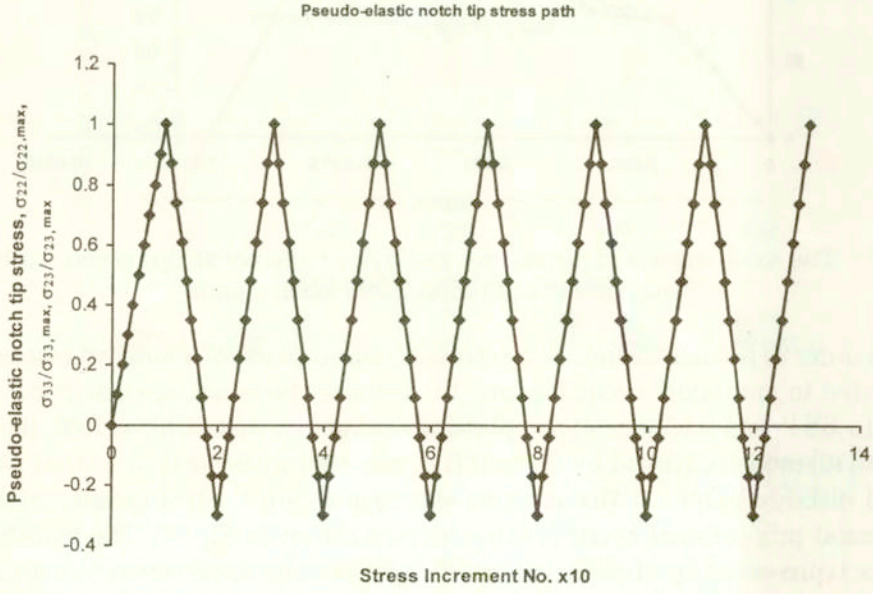

FIG. 9. The multiaxial cyclic loading history.

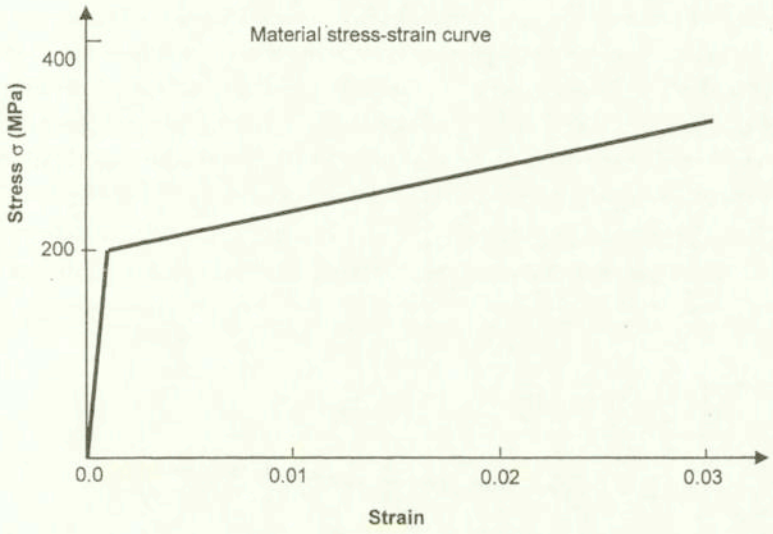

FIG. 10. The two linear segments material stress-strain curve used for the analysis of strain and stresses under the multiaxial cyclic loading path.

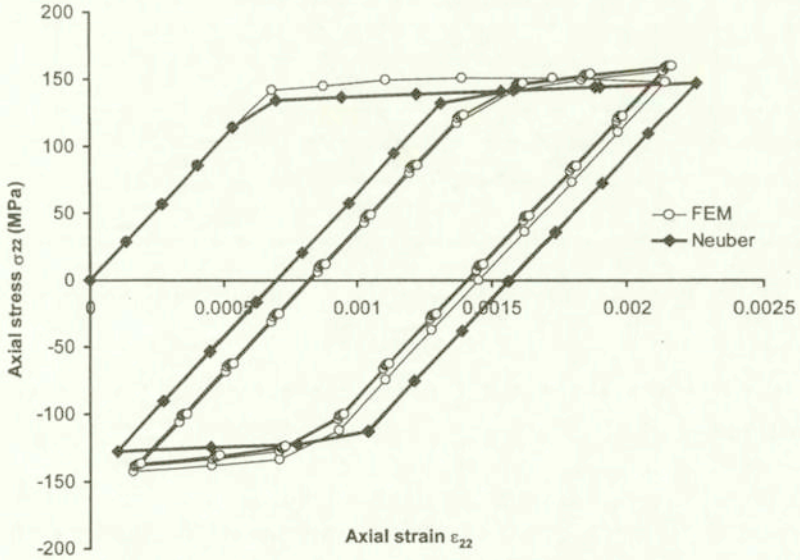

FIG. 11. The axial stress and strain, σ_{22} and ε_{22}, induced by the multiaxial cyclic loading path.

The material stress-strain curve was that one composed of two linear segments (Fig. 10) defined by $\varepsilon - \sigma$ coordinates of the transition points, i.e. $0 - 0$, $0.001 - 200$ MPa and $0.06135 - 450$ MPa. The elastic constants were the same as previously. The elastic-plastic notch tip strain-stress histories are shown in Figs. 11 and 12. It can be noticed that both the axial and the shear strain were over-predicted by the Neuber-based approach, similarly to many previous reports concerning the Neuber rule. However, the over-prediction might be acceptable in many practical applications, where the time available for the analysis is limited. It is worth mentioning that the ABAQUS program required 30 hours CPU time while the total strain energy density-based calculations were completed within a fraction of a second for the same number of load increments run on the same computer.

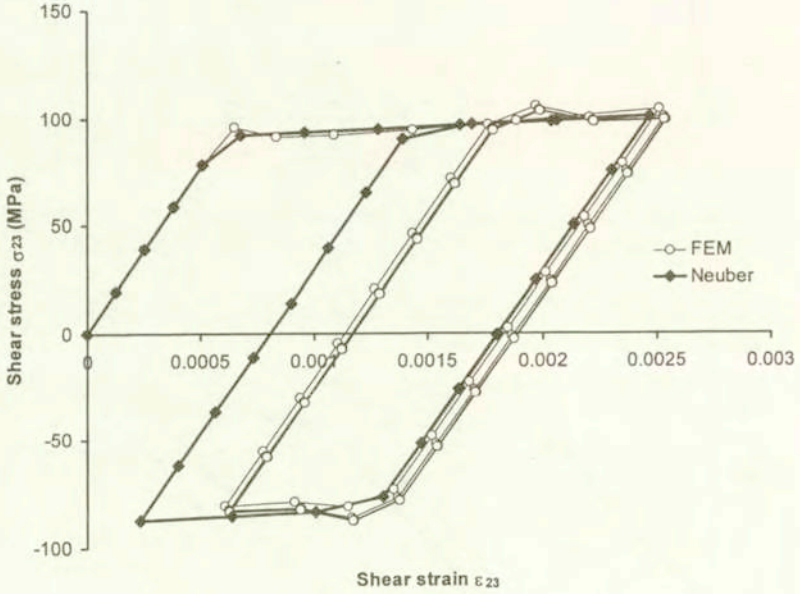

FIG. 12. The shear stress and strain, σ_{23} and ε_{23}, induced by the multiaxial cyclic loading path.

9. Conclusions

Two methods for calculating elastic-plastic notch tip strains and stresses induced by multiaxial loading paths have been proposed. The methods have been formulated using both the total strain energy density and the strain energy density relationships. It has been found that the generalized Neuber's rule, which represents the equality of the total strain energy density at the notch tip, gives an upper bound estimate for the elastic-plastic notch tip strains. The method

has been verified by comparison with the finite element data obtained for non-proportional loading path and nonlinear stress-strain material model. The accuracy of the proposed method was satisfactory, particularly where the notch tip stresses are of primary importance.

The calculated notch tip strains and stresses can be subsequently used for estimating the fatigue damage and life prediction for multiaxial cyclic loading histories.

References

1. H. NEUBER, *Theory of stress concentration shear strained prismatic bodies with arbitrary non-linear stress-strain law*, ASME Journal of Applied Mechanics, **28**, 544–550, 1961.
2. K. MOLSKI and G. GLINKA, *A method of elastic-plastic stress and strain calculation at a notch root*, Material Science and Engineering, **50**, 93–100, 1981.
3. A. MOFTAKHAR, A. BUCZYNSKI and G. GLINKA, *Calculation of elasto-plastic strains and stresses in notches under multiaxial loading*, International Journal of Fracture, **70**, 357–373, 1995.
4. M. N. K. SINGH, G. GLINKA and R. N. DUBEY, *Elastic-plastic stress-strain calculation in notched bodies subjected to non-proportional loading*, International Journal of Fracture, **76**, 1, 39–60, 1996.
5. T. SEEGER and M. HOFFMAN, *The use of Hencky's equations for the estimation of multiaxial elastic-plastic notch stresses and strains*, Report No. FB-3/1986, Technische Hochschule Darmstadt Germany 1986.
6. M. E. BARKEY, D. F. SOCIE and K. J. HSIA, *A yield surface approach to the estimation of notch strains for proportional and non-proportional cyclic loading*, ASME Journal of Engineering Materials and Technology, **116**, 173–180, 1994.
7. A. A. MOFTAKHAR, *Calculation of time-independent and time-dependent strains and stresses in notches*, Doctoral Dissertation, University of Waterloo, Department of Mechanical Engineering, Waterloo, Ontario, Canada 1994.
8. C.-C. CHU, *Incremental multiaxial neuber correction for fatigue analysis*, International Congress and Exposition, SAE Technical Paper No. 950705, Detroit 1995.
9. N. K. SINGH, A. BUCZYNSKI and G. GLINKA, *Notch stress-strain analysis and life prediction in multiaxial fatigue*, Proceedings of the Int. Conference on 'Fatigue Design 95', G. MARQUIS *et al.* [Eds.], Sept. 5-8, Helsinki 1995.
10. Z. MRÓZ, *On the Description of Anisotropic Workhardening*, Journal of Mechanics and Physics of Solids, **15**, 163–175, 1967.
11. Y. S. GARUD, *A new approach to the evaluation of fatigue under multiaxial loading*, Journal of Engineering Materials and Technology, ASME, **103**, 118–125, 1981.

Received February 24, 2000; revised version July 5, 2000.